

Evolution of Transient Low-Mass X-ray Binaries to Redback Millisecond Pulsars

Kun Jia¹ and Xiang-Dong Li^{1,2}

¹*Department of Astronomy, Nanjing University, Nanjing 210046, China*

²*Key laboratory of Modern Astronomy and Astrophysics (Nanjing University), Ministry of Education, Nanjing 210046, China*

lixd@nju.edu.cn

ABSTRACT

Redback millisecond pulsars (hereafter redbacks) are a sub-population of eclipsing millisecond pulsars in close binaries. The formation processes of these systems are not clear. The three pulsars showing transitions between rotation- and accretion-powered states belong to both redbacks and transient low-mass X-ray binaries (LMXBs), suggesting a possible evolutionary link between the them. Through binary evolution calculations, we show that the accretion disks in almost all LMXBs are subject to the thermal-viscous instability during certain evolutionary stages, and the parameter space for the disk instability covers the distribution of known redbacks in the orbital period - companion mass plane. We accordingly suggest that the abrupt reduction of the mass accretion rate during quiescence of transient LMXBs provides a plausible way to switch on the pulsar activity, leading to the formation of redbacks, if the neutron star has been spun up to be an energetic millisecond pulsar. We investigate the evolution of redbacks, taking into account the evaporation feedback, and discuss its possible influence on the formation of black widow millisecond pulsars.

Subject headings: binaries: eclipsing - stars: evolution - stars: neutron - X-rays: binaries - pulsars: X-rays

1. Introduction

Millisecond pulsars (MSPs) are a population of neutron stars (NSs) with fast spins and weak magnetic fields (Backer et al. 1982). They are thought to have evolved from low-mass X-ray binaries (LMXBs) (Bhattacharya & van den Heuvel 1991, for a review). The

discovery of coherent millisecond X-ray pulsations from several NSs in LMXBs strongly confirms this theoretical expectation (Patruno & Watts 2012, and references therein). More recent observations demonstrate transitions between a rotation- and an accretion-powered state in three systems, i.e., PSR J1023+0038 (Archibald et al. 2009; Stappers et al. 2014; Patruno et al. 2014), PSR J1824–2452I/IGR J18245–2452 (Papitto et al. 2013), and XSS J12270–4859 (de Martino et al. 2010, 2013; Roy et al. 2014).

Black widow and redback MSPs (hereafter redbacks) are two sub-populations of eclipsing MSPs with orbital periods $P_{\text{orb}} \lesssim 1$ day (Roberts 2013, for a recent review). While redbacks have relatively more massive companions ($0.2 M_{\odot} \lesssim M_2 \lesssim 0.4 M_{\odot}$), the companion masses in black widow binaries are significantly lower ($0.02 M_{\odot} \lesssim M_2 \lesssim 0.05 M_{\odot}$) (Fruchter et al. 1988; Stappers et al. 1996). The most striking feature of both types of binaries is their regular radio eclipses around superior conjunction (Roberts 2013, and references therein). These deep eclipses indicate a low-density, highly-ionized gas cloud wrapping the companions, but the origin of the eclipsing material is not clear. Consider the compact orbits and the fact that they are associated with γ -ray sources, the eclipsing material could originate from the companions evaporated by the high-energy particles from the MSPs (van den Heuvel & van Paradijs 1988; Ruderman et al. 1989a). Alternatively, the nearly Roche-lobe (RL) filling companions (van Kerkwijk et al. 2011; Deller et al. 2012) suggest that there may be Roche-lobe overflow (RLOF) in these binaries, and the overflowing matter is stopped and blown away by the MSP’s radiation pressure at the inner Lagrangian point (Ruderman et al. 1989a; Burderi et al. 2001, 2002).

Notably, all the three transitional MSPs discovered so far are redbacks, which have a currently known population of 17 sources (see Table 1 in Smedley et al. 2015). With a systematic X-ray study of eight nearby redbacks, Linares (2014) defined three (pulsar, disk, and outburst) states according to their X-ray luminosities. In the pulsar state, the X-ray luminosities are in the range of $10^{31} \text{ ergs} < L_X < 4 \times 10^{32} \text{ erg s}^{-1}$, and they exhibit radio eclipses and pulsations (Archibald et al. 2010). In the disk state with $4 \times 10^{32} \text{ ergs}^{-1} < L_X < 10^{34} \text{ erg s}^{-1}$, the disk lines can be detected in the optical band accompanied with fast bimodal switching in X-rays (Ferrigno et al. 2014; Linares et al. 2014). The (full accretion) outburst state with $L_X > 10^{34} \text{ erg s}^{-1}$ has been detected only in PSR J1824–2452I so far (Papitto et al. 2013).

In the general picture of the NS–accretion disk interaction, the inner radius of a geometrically thin accretion disk is truncated at the magnetospheric radius where the energy of the NS magnetic field equals the kinetic energy of the infalling matter in the disk (Pringle & Rees 1972): $R_m \simeq \mu^{4/7} (2GM_{\text{NS}})^{-1/7} \dot{M}^{-2/7}$, where μ is the magnetic moment of the NS, M_{NS} the NS mass, \dot{M} the accretion rate, and G the gravitational constant. With a

high enough accretion rate, the magnetospheric radius can be inside the corotation radius at which the Keplerian angular velocity in the disk is equal to the angular velocity Ω_{NS} of the NS: $R_{\text{co}} = (GM_{\text{NS}}/\Omega_{\text{NS}}^2)^{1/3}$, and the accreting matter can be channeled by the field lines to reach the NS surface. If the accretion rate is reduced and the magnetospheric radius expands outside the corotation radius, a significant fraction of the accreting matter may be ejected from the system with the so-called propeller effect (Illarionov & Sunyaev 1975). Furthermore, if the accretion rate is so low that the magnetospheric radius is beyond the light cylindrical radius (where the corotating velocity matches the speed of light, $R_{\text{LC}} = c/\Omega_{\text{NS}}$), the disk is disrupted and a radio pulsar switches on. So, to account for the mass outflows and transitional behavior in redbacks, we require a significant variation in the mass accretion rate during the binary evolution.

Based on this argument, three models have been proposed for the formation of redbacks by invoking interrupted mass transfer processes. Below we briefly review these models.

1. *The disrupted magnetic braking (MB) model*

Mass transfer in short orbital period LMXBs is driven by angular momentum loss (AML) due to MB and gravitational radiation (GR). When its mass decreases to around $0.2\text{--}0.3 M_{\odot}$, the donor becomes fully convective and the MB-induced AML is greatly reduced, leading to RL decoupling (e.g. Spruit & Ritter 1983). As a result, the mass transfer is temporarily halted. Chen et al. (2013) assumed that a MSP then switches on and begins to evaporate its companion star with high-energy radiation. They investigated the subsequent binary evolution, and showed that adopting different values of the evaporation efficiency could account for the formation of both black widows and redbacks. In this model it is hard to explain a few redbacks with relatively large companion masses ($\sim 0.5 M_{\odot}$) and long orbital periods ($\gtrsim 0.5$ day). The authors suggested that these systems may have been temporarily detached earlier for some reasons, then turned into the evaporation stage with a relatively massive companion star.

2. *The irradiation-induced cyclic mass transfer model*

When the donor star in a LMXB is irradiated by the X-rays from the accreting NS, its intrinsic luminosity can be blocked by irradiation (Podsiadlowski 1991; Hameury et al. 1993). Due to the thermal relaxation of the convective envelope of the donor star, the secular mass transfer could be unstable under some conditions, cycling between low and high states (Ritter et al. 1996; King et al. 1995, 1996; Büning & Ritter 2004). Benvenuto et al. (2014, 2015) found that this irradiation instability and cyclic mass transfer processes are popular during the evolution of contracting LMXBs, and they suggested that redbacks may be formed during the low state of the mass transfer. In this scenario, the redback companions should

almost fill their RL. By considering the evaporation due to the MSP’s wind/radiation, they found that black widows can descend from redbacks, but not all redbacks evolve into black widows. A caveat is that this model may not work in transient LMXBs, in which the mass transfer cycles would be suppressed due to intermittent irradiation (Ritter 2008).

3. *The accretion-induced collapse (AIC) model*

Smedley et al. (2015) suggested that redbacks may be formed during the AIC of a white dwarf (WD) in cataclysmic variable (CV)-like systems besides the traditional recycling scenarios. At the time of AIC, the companion star becomes detached from its RL because of the orbital expansion caused by sudden gravitational mass loss. The mass transfer halts and the newborn MSP starts to ablate its companion. Like the cyclic mass transfer model, the AIC model can reproduce all redbacks in the $M_2 - P_{\text{orb}}$ plane. However, Ablimit & Li (2015) pointed out that it is difficult or impossible to produce the requisite occurrence of AIC in traditional CVs, unless irradiation-excited wind from the donor star is also taken into account.

More recently, channeled accretion was detected in PSR J1023+0038 (Archibald et al. 2015), which is actually an accreting millisecond X-ray pulsar (AMXP). Unlike other AMXPs, this channeled accretion was discovered at a very low X-ray luminosity $L_X < 10^{34}$ erg s $^{-1}$, which challenges the traditional accretion-propeller theory (Archibald et al. 2015; Bogdanov et al. 2014). Similar phenomenon has also been discovered in XSS J12270–4859 (Papitto et al. 2015). Adding PSR J1824–2452I as a typical AMXP in the outburst state (Papitto et al. 2013), we note that all the three transitional redbacks exhibit as AMXPs at the disk or outburst state. As we know, all the AMXPs are transient systems (Patruno & Watts 2012), likely caused by the thermal-viscous instability in the accretion disks (see Lasota 2001, for a review). It is also noted that, all NS-LMXBs are subject to the disk instability either with evolved companions (King et al. 1997) or with low main-sequence (MS) companions after the cessation of MB, as we show below. Observationally nearly half of the LMXBs in the Galactic disk are transient sources (Ritter & Kolb 2003; Knevitt et al. 2014). Based on these features, we consider the thermal-viscous disk instability as a possible mechanism for the formation of redbacks, and investigate their evolutionary sequences.

The rest of this paper is organized as follows. In Section 2 we briefly introduce the binary evolution model. Our main results on the parameter space of the disk instability and its effect on the LMXB evolution are presented in Sections 3 and 4, respectively. They are then discussed in Section 5 and summarized in Section 6.

2. Method

We calculate the LMXB evolution with an updated version (7624) of the Modules for Experiments in Stellar Astrophysics (MESA) (Paxton et al. 2011, 2013, 2015). The binary is initially composed of a NS (of mass M_1) and a zero-age main-sequence (ZAMS) companion star (of mass M_2) with solar chemical compositions. We use the Eggleton (1983) formula to calculate the effective RL radius of the companion (or donor) star,

$$\frac{R_{L,2}}{a} = \frac{0.49q^{-2/3}}{0.6q^{-2/3} + \ln(1 + q^{-1/3})}, \quad (1)$$

where $q = M_1/M_2$ is the mass ratio and a is the orbital separation. To calculate the mass transfer rate via RLOF we adopt the Ritter scheme (Ritter 1988; Paxton et al. 2015) in the code, which takes into account the finite scale height of the stellar atmosphere of the donor,

$$-\dot{M}_2 = \dot{M}_0 \exp\left[\frac{R_2 - R_{L,2}}{H_P/\gamma(q)}\right]. \quad (2)$$

Here \dot{M}_0 depends on the mass ratio, the density at the donor’s photosphere and its effective temperature, R_2 is the donor’s radius, H_P is the pressure scale height of the atmosphere, and γ is a function of q . The rate of AML during the evolution consists of three parts:

$$\dot{J} = \dot{J}_{\text{GR}} + \dot{J}_{\text{ML}} + \dot{J}_{\text{MB}}. \quad (3)$$

The first term \dot{J}_{GR} on the right hand side is the rate of GR-induced AML given by (Landau & Lifshitz 1975),

$$\dot{J}_{\text{GR}} = -\frac{32}{5} \frac{G^{7/2}}{c^5} \frac{M_1^2 M_2^2 (M_1 + M_2^{1/2})}{a^{7/2}}. \quad (4)$$

with c the speed of light. The second term is due to the mass loss from the system. We assume that a fraction (β) of the transferred mass is accreted by the NS and the rest is ejected out of the system by isotropic winds, taking away the specific AM of the NS,

$$\dot{J}_{\text{ML}} = -(1 - \beta) \dot{M}_2 \left(\frac{M_2}{M_1 + M_2}\right)^2 a^2 \omega, \quad (5)$$

where ω is the angular velocity of the binary orbit. We also assume that the accretion rate \dot{M}_1 is limited by the Eddington critical rate,

$$\dot{M}_{\text{Edd}} = 3.6 \times 10^{-8} \left(\frac{M_1}{1.4M_\odot}\right) \left(\frac{0.1}{GM_1/R_1 c^2}\right) \left(\frac{1.7}{1 + X}\right) M_\odot \text{yr}^{-1}, \quad (6)$$

where X is the hydrogen abundance and R_1 is the NS radius, taken to be 10^6 cm. Our previous work shows that the value of β does not significantly affect the evolutionary tracks of LMXBs (Jia & Li 2014), so here we fix its value to be 0.5. Thus, $\dot{M}_1 = \min(-\dot{M}_2/2, \dot{M}_{\text{Edd}})$.

The last term in Eq. (3) represents the AML due to MB, for which we adopt the standard formula (Verbunt & Zwaan 1981; Rappaport et al. 1983),

$$\dot{J}_{\text{MB}} = -3.8 \times 10^{-30} M_2 R_2^4 \omega^3 \text{ dyn cm.} \quad (7)$$

We assume that MB is reduced when the star’s convective envelope is very thin, and add an ad hoc factor to \dot{J}_{MB} (Podsiadlowski et al. 2002),

$$\exp(-0.02/q_{\text{conv}} + 1) \quad (\text{if } q_{\text{conv}} < 0.02),$$

where q_{conv} is the mass fraction of the surface convective envelope. We also terminate MB when the central stellar radiative zone vanishes.

The accretion disk in a LMXB becomes thermally and viscously unstable when the mass transfer rate drops below a critical value. Then the LMXB may appear as a transient source experiencing limit cycles between short outbursts and long quiescent intervals with a duty cycle $d \sim 0.001 - 0.1$ (King et al. 2003). Here we adopt the critical mass transfer rate for an irradiated disk given by (Dubus et al. 1999),

$$\dot{M}_{\text{cr}} \simeq 3.2 \times 10^{-9} \left(\frac{M_1}{1.4M_{\odot}} \right)^{0.5} \left(\frac{M_2}{1.0M_{\odot}} \right)^{-0.2} \left(\frac{P_{\text{orb}}}{1.0 \text{ d}} \right)^{1.4} M_{\odot} \text{yr}^{-1}. \quad (8)$$

Once $\dot{M}_1 < \dot{M}_{\text{cr}}$, we simply assume that there is no accretion during quiescence, and the matter flow accretes at a rate of $\dot{M}_1 = \min(-\dot{M}_2/2d, \dot{M}_{\text{Edd}})$ during outbursts. Here we set the duty cycle $d = 0.01$ throughout this paper. Since the evolution time steps in the code are usually much longer than the disk outburst cycle time, the average mass transfer rate from the donor star actually remains the same as in the case of stable disk accretion, but the accreted mass by the NS is considerably reduced.

3. The parameter space for unstable disks

We calculate the evolution of a grid of LMXBs with a $1.35 M_{\odot}$ NS and a donor star of initial mass $M_{2,i} = 1.0, 1.5, \text{ and } 2.0 M_{\odot}$. The initial orbital periods $P_{\text{orb},i}$ is set to range from ~ 0.4 day to ~ 20 days, to cover the evolution of CV-like, ultra-compact and wide LMXBs (Deloye 2008).

We show some of the calculated evolutionary tracks in the $M_2 - P_{\text{orb}}$ plane (Fig. 1). From left to right, the three panels correspond to $M_{2,i} = 1.0, 1.5, \text{ and } 2.0 M_{\odot}$, respectively. In each panel the green solid and red dotted lines represent the mass transfer processes with stable

and unstable accretion disks, respectively. The black dashed lines denote the stage of RL detachment (i.e., without mass transfer). The asterisk on each evolutionary track indicates that the accreted mass reaches $0.1 M_{\odot}$, a typical amount to spin up a NS to millisecond periods (Lipunov & Postnov 1984; Zhang et al. 2011; Tauris et al. 2012). The dot-dashed line shows the relation between the orbital period and the (WD) core mass of the donor (i.e., $P_{\text{orb}} - M_{\text{WD}}$ relation) after Case B mass transfer (Joss et al. 1987; Rappaport et al. 1995; Tauris & Savonije 1999; Lin et al. 2011; Jia & Li 2014). Here we use the calculated results of Lin et al. (2011). The two brown dashed lines give the orbital periods when the donor star is on ZAMS and terminal-age main-sequence (TAMS). They are obtained by combining the orbital period - donor radius relation (Rappaport et al. 1995)

$$P_{\text{orb}} = 20G^{-1/2}R_2^{3/2}M_2^{-1/2}, \quad (9)$$

with the mass - radius relations (Demircan & Kahraman 1991) for ZAMS stars,

$$R_2 \simeq \begin{cases} 0.89(M_2/M_{\odot})^{0.89} R_{\odot} & (\text{for } M_2 < 1.66M_{\odot}) \\ 1.01(M_2/M_{\odot})^{0.57} R_{\odot} & (\text{for } M_2 > 1.66M_{\odot}) \end{cases}, \quad (10)$$

and for TAMS stars,

$$R_2 \simeq \begin{cases} 2.00(M_2/M_{\odot})^{0.75} R_{\odot} & (\text{for } M_2 < 1.66M_{\odot}) \\ 1.61(M_2/M_{\odot})^{0.83} R_{\odot} & (\text{for } M_2 > 1.66M_{\odot}) \end{cases}, \quad (11)$$

respectively.

In Fig. 1 we also plot the known redbbacks with open diamonds and squares in the Galactic field (field redbbacks) and globular clusters (GC redbbacks) listed in Smedley et al. (2015), respectively. Note that we have recalculated their masses by assuming a NS mass of $1.35 M_{\odot}$ instead of $1.25 M_{\odot}$ in Smedley et al. (2015).

Iben et al. (1995) divided the LMXB evolution into 7 cases according to the evolutionary state of the donor star and the mass transfer mode. Our calculations demonstrate that the LMXBs are persistent, i.e., non-transient, in the following cases when the mass transfer is driven by (1) MB for CV-like LMXBs with MS donors; (2) thermal expansion of a massive evolved donor; and (3) GR in ultra-compact systems with $P_{\text{orb}} \lesssim 1$ hour.

Figure 2 shows some illustrative examples of mass transfer rates in the black solid lines. We divide the evolutionary tracks into three types according to whether the initial orbital period being longer or shorter than, or close to the so-called the "bifurcation period" (Pylyser & Savonije 1988, 1989). The red dashed lines depict the critical mass transfer rates for comparison.

The bottom row of Fig. 2 shows the evolutions of contracting systems. In the case of $M_{2,i} = 1.0 M_{\odot}$ and $P_{\text{orb},i} = 0.4$ day, the mass transfer begins when the companion star is still unevolved, so MB dominates the AML and the mass transfer rate is initially above \dot{M}_{cr} . When the donor becomes fully convective, MB stops and AML is solely caused by GR, the mass transfer rate drops down below \dot{M}_{cr} and the binary becomes transient. When $M_{2,i} = 1.5 M_{\odot}$ and $P_{\text{orb},i} = 0.5$ day, in the initial stage of the mass transfer, MB takes no effect because the donor has a radiative envelope, and the accretion disk is unstable because of the low mass transfer rate. When the stripped donor star has developed a convective envelope, MB starts to work and the binary becomes persistent. The following evolution is similar to the case of $M_2 = 1.0 M_{\odot}$. For a more massive donor with $M_{2,i} = 2.0 M_{\odot}$ and $P_{\text{orb},i} = 0.55$ day, mass transfer proceeds rapidly on a thermal timescale (Podsiadlowski et al. 2002; Lin et al. 2011). After that the mass transfer rate decays. When the donor mass is comparable to the NS mass before MB takes effect, the mass transfer rate drops below \dot{M}_{cr} and produces a dip. The subsequent evolution is also similar to the previous cases.

The evolutions of widening binaries are shown in the top row of Fig. 2. When $M_{2,i} = 1.0 M_{\odot}$ and $P_{\text{orb},i} = 20.0$ days, different from the contracting binaries, the donor star is evolved and the mass transfer is driven by the stellar expansion due to shell burning on the red giant branch, which results in a expanding orbit and a much higher \dot{M}_{cr} . Accordingly, we see that the mass transfer rate is always below \dot{M}_{cr} . In the cases of $M_{2,i} = 1.5 M_{\odot}$, $P_{\text{orb},i} = 10.0$ days, and $M_{2,i} = 2.0 M_{\odot}$, $P_{\text{orb},i} = 2.0$ days, a mass transfer rate above $10^{-7} M_{\odot} \text{yr}^{-1}$ is reached at the initial stage. As the evolution proceeds, the mass transfer rate descends while \dot{M}_{cr} increases due to orbital expansion, so the disks become unstable for wider systems. The final evolutionary products are MSP-He WD binaries.

The middle row of Fig. 2 presents examples just between contracting and widening binaries, with the final orbital periods around 1 day. At the beginning of mass transfer, the donor star is on the MS, similar as in contracting binaries, and the accretion disk is stable. Then the mass transfer rate gradually declines to be below \dot{M}_{cr} , due to the slight expansion of the donor during the MS evolution. For $M_{2,i} = 2.0 M_{\odot}$, there is a spike in the mass transfer rate at $M_2 \sim 0.5 - 0.6 M_{\odot}$, which indicates the end of the MS evolution. The donor star evolves rapidly to pass through the Hertzsprung gap, when its H-exhausted core mass exceeds the Schönberg-Chandrasekhar limit. In the case of $M_{2,i} = 1.0 M_{\odot}$, there is not such a spike since the Schönberg-Chandrasekhar limit is irrelevant for lower mass ($< 1.1 M_{\odot}$) stars, in which electron degeneracy pressure dominates the He core. These stars can gradually transit from central- to shell-hydrogen burning with no Hertzsprung gap in the H-R diagram.

Go back to Fig. 1, we see that the parameter space for the occurrence of the disk

instability covers the distribution of known redbacks. If MSP activity switches on during the quiescent phase of LMXBs (as observed in the three transitional pulsars), it may lead to the formation of redbacks.

4. Evolution with evaporation

Considering the fact that the evaporation processes can be rather complicated, here we adopt the simple picture that, when a NS in a LMXB spins at millisecond periods and the mass transfer rate declines to be low enough, a radio pulsar will turn on and prevent further accretion (Ruderman et al. 1989a; Burderi et al. 2001, 2002); meanwhile, part of the spin-down energy is used to evaporate the companion star (van den Heuvel & van Paradijs 1988). Therefore, we assume that evaporation in LMXBs takes place once the following two conditions are satisfied: (1) during the mass transfer phase, a NS has accreted at least $0.1M_{\odot}$ mass to be recycled as a MSP, and (2) the mass accretion rate decreases significantly, either due to a decrease in the mass transfer rate or because the accretion disk becomes unstable.

We note that, if the disk is in an unstable state, evaporation can take place effectively simultaneously as far as the evolution time steps in the code are concerned. Our calculations show that there can be either RLOF or not along with evaporation, depending on the subsequent evolution of the stellar radius and the RL radius (see discussion in next section). In the case of evaporation accompanied with RLOF, we assume that the accretion disk is outside the light cylinder (at ~ 100 km) during the quiescent phase, then the NS does not accrete and acts as a radio pulsar. The material in the inner disk is blown away from the binary, but most of the transferred material from the companion star continues to accumulate in the outer region of the disk ($\sim 10^2 - 10^6$ km). When the disk switches to the outburst phase, the disk material rapidly accretes onto the NS and the pulsar shuts off. Since the accretion rates during outbursts are generally super-Eddington, most of the material is also assumed to be lost from the binary. Thus, considering the long evolution time steps in the calculation, we assume that almost all of the transferred matter is ejected, taking away the specific AM of the NS.

In the mean time, to explore the evaporation effect on the secular evolution, we assume that evaporation proceeds at a rate (van den Heuvel & van Paradijs 1988; Stevens et al. 1992),

$$\dot{M}_{2,\text{evap}} = -\frac{f}{2v_{2,\text{esc}}^2}L_{\text{p}}\left(\frac{R_2}{a}\right)^2, \quad (12)$$

where $v_{2,\text{esc}}$ is the escape velocity at the surface of the companion star, $L_{\text{p}} = 4\pi^2I\dot{P}/P^3$ is the NS's spin-down luminosity, and f is the efficiency of evaporation. Here I , P , and \dot{P} are

the moment of inertia, the spin period and its derivative of the NS, respectively. We assume that the evaporating material takes away the specific AM of the companion star.

When a radio pulsar turns on, we assume that its spin evolves following the standard magnetic dipole radiation model with a constant braking index $n = 3$ (Shapiro & Teukolsky 1983), and neglect the change in P due to accretion during outbursts because of their short duration. We take typical values of the initial spin period $P = 3$ ms, period derivative $\dot{P} = 1.0 \times 10^{-20} \text{ ss}^{-1}$, and moment of inertia $I = 10^{45} \text{ gcm}^2$.

Similar to Fig. 1, we show a series of evolutionary sequences in Fig. 3 taking into account the evaporation effect, where we set the efficiency factor $f = 0.1$. The beginning of evaporation is denoted with a pentagram on each evolutionary track. In some cases it starts due to a drop of the mass transfer rate when the companion mass is comparable with the NS mass, as shown in Fig. 4. Comparison between Figs. 1 and 3 demonstrates that evaporation can considerably alter the evolution of LMXBs, in broad agreement of Chen et al. (2013) and Smedley et al. (2015). However, the orbital period evolution in Fig. 3 is more flattened than in Chen et al. (2013) and Smedley et al. (2015), since we take account of the AML due to the evaporating material. This feature can be illustrated as follows. The orbital angular momentum of the binary is

$$J = M_1 M_2 \left(\frac{Ga}{M} \right)^{1/2}, \quad (13)$$

where $M = M_1 + M_2$ is the total mass. Logarithmically differentiating the above equation with respect to time gives the change in the orbital separation due only to evaporative mass loss from the companion star,

$$\frac{\dot{a}}{a} = -\frac{2\dot{M}_2}{M_2} \left(1 - \frac{M_2}{2M} - \alpha_{\text{evap}} \frac{M}{M_1} \right), \quad (14)$$

where α_{evap} is the specific AM of the evaporative wind in units of the binary's specific AM. If the evaporative wind carries the specific AM of the companion star, we have

$$\frac{\dot{a}}{a} = -\frac{2\dot{M}_2}{M_2} \left(1 - \frac{M_2}{2M} - \frac{M_1}{M} \right). \quad (15)$$

In the limit where $M_2 \ll M_1$, Eq. (14) becomes

$$\frac{\dot{a}}{a} \simeq -\frac{2\dot{M}_2}{M_2} (1 - \alpha_{\text{evap}}). \quad (16)$$

Thus if $\alpha_{\text{evap}} \rightarrow 0$ (i.e., no AML due to evaporative mass loss) the orbit will expand considerably, while if $\alpha_{\text{evap}} \rightarrow 1$ the orbit will not expand at all.

In Fig. 4 we display how evaporation influences the binary evolution for the three cases in Fig. 2. The black solid and blue dotted lines represent the RLOF mass transfer rate and the evaporative wind loss rate, respectively. We start with the CV-like contracting systems as shown in the bottom row of Fig. 4. Here evaporation takes place when the donor star decouples from its RL due to the cessation of MB, same as in Chen et al. (2013), but the orbital periods of the resultant redbacks are around 0.1 day, different from in the range of $\sim 0.1 - 1$ day in Chen et al. (2013). As mentioned before, for donor stars with mass $M_{2,i} = 1.5$ and $2.0 M_{\odot}$, there exists a dip in the mass transfer rate (which is below \dot{M}_{cr}) before MB operates. Evaporation may also take place at this time if the NS has accreted enough mass to be recycled as a MSP. This suggests the possibility of detecting redbacks with $M_2 \gtrsim 1.0 M_{\odot}$. When the donor’s mass decreases to $\sim 1.0 M_{\odot}$, its convective envelope is developed and MB starts to operate, then the mass transfer increases and evaporation stops. It will start again when the companion star is detached from its RL.

The top row of Fig. 4 presents the evolutions in the case of widening systems. Mass accretion of NSs is generally inefficient in these systems, because of both short evolutionary time and transient behavior, so the NSs may not be fully recycled. Nevertheless, for relatively massive donor stars such as $M_{2,i} = 2.0 M_{\odot}$, the NS can still accrete enough mass during the intermediate-mass X-ray binary phase (Shao & Li 2012), and we may expect redbacks with subgiant companions and orbital periods up to tens of days. In the case of $M_{2,i} = 2.0 M_{\odot}$ and $P_{\text{orb},i} = 2.0$ days, at the end of evolution, the binary undergoes a short-lived ($\sim 10^3$ yrs) episode of additional RLOF as a result of the hydrogen shell flashes on the proto-WD (e.g., Antoniadis 2014). The resultant MSP-He WD binaries follow the $P_{\text{orb}} - M_{\text{WD}}$ relation because the companions are generally RL filling. However, all redbacks discovered so far are in relatively compact orbits with period less than ~ 1.5 day, so there seems to be a gap between observations and theoretical expectation, and we will return to this point later.

In the middle row of Fig. 4 the orbital periods of redbacks are distributed around 0.1 – 1 day, close to the bifurcation period. Different from the case of the contracting systems, the mass transfer rate drops below \dot{M}_{cr} before MB ceases. Along with evaporation, the donor star keeps overflowing its RL. The mass transfer rate declines but the total mass loss rate of the donor star increases. When the donor star approaches the end of nuclear evolution, it cannot adjust immediately to fill its RL, RLOF terminates and evaporation starts to dominate the mass loss. In this case the redback companions may either fill or underfill their RLs, and the finally formed MSP-He WD binaries may slightly deviate from the $P_{\text{orb}} - M_{\text{WD}}$ relation.

In summary, evaporation can considerably influence the secular binary evolution, especially for relatively compact systems. The switch-on of radio activity and start of evaporation

are caused by the transient behavior of LMXBs, as well as disrupted MB. The predicted parameter space is consistent with the distribution of known redbacks in the $M_2 - P_{\text{orb}}$ plane.

5. Discussion

(1) Transitional pulsars and redbacks

We have shown that transient LMXBs that harbor energetic MSPs may lead to the formation of redbacks. The three transitional pulsars clearly demonstrate the close relation between redbacks and transient AMXPs. Moreover, Papitto et al. (2015) found a very similar spin distribution between AMXPs and eclipsing MSPs, suggesting that the two groups belong to a common class at the same evolutionary epoch. This is also consistent with our hypothesis that both redbacks and AMXPs originate from transient LMXBs. The related questions are: which redbacks can experience transitions to the disk accretion state, and why don't all transient AMXPs show radio pulsations during quiescence?

Based on the statistics of the current sample, Linares et al. (2014) divided redbacks into two groups according to their luminosities during the pulsar state, and suggested that the bright ones with X-ray luminosity above 10^{32} ergs $^{-1}$ are promising candidates to develop accretion disks. Considering the fact that disk accretion always requires RLOF, obviously redbacks with a lobe-filling companion are likely to experience transitions to the accretion state, while those with a underfilling companion should stay in the radio pulsar state. Our results show that the redback companions can either fill or underfill their RLs, depending on how much mass and AM are lost with evaporation. The condition can be briefly analyzed as follows. For stable mass transfer via RLOF, from the condition

$$\frac{\dot{R}_2}{R_2} = \frac{\dot{R}_{L,2}}{R_{L,2}}, \quad (17)$$

one can derive the following formula for the mass transfer rate (Rappaport et al. 1983)

$$-\frac{\dot{M}_2}{M_2} = \frac{\frac{1}{2} \left(\frac{\dot{R}_2}{R_2} \right)_{\text{evol,therm}} - \left(\frac{\dot{J}}{J} \right)_{\text{MB,GR}}}{\frac{5}{6} + \frac{\xi_{\text{ad}}}{2} - \frac{1 - \beta}{3(1 + q)} - \frac{(1 - \beta)\alpha(1 + q) + \beta}{q}}, \quad (18)$$

where $(\dot{R}_2/R_2)_{\text{evol,therm}}$ represents the change in the companion star's radius under thermal or nuclear evolution, $\dot{J}_{\text{MB,GR}}$ is the AML rate due to MB and GR, ξ_{ad} is the adiabatic radius-mass exponent, β is the fraction of the mass overflowing from the donor star that is retained

by the NS, and α is the specific AM of the lost material in units of the binary’s specific AM. If we consider RLOF and evaporation simultaneously, we can divide the total mass loss rate of the donor into two parts, $\dot{M}_2 = \dot{M}_{2,\text{RL}} + \dot{M}_{2,\text{evap}}$, where $\dot{M}_{2,\text{RL}}$ and $\dot{M}_{2,\text{evap}}$ are the mass loss rates through RLOF and evaporative wind, respectively. Assuming that the mass transfer is partially non-conservative and the winds from the NS and the donor take away the specific AM of α_{RL} and α_{evap} , respectively, we can rewrite Eq. (18) to be,

$$\frac{|\dot{M}_{2,\text{RL}}|}{M_2} = \frac{N}{D}, \quad (19)$$

where

$$N = \left(\frac{\dot{R}_2}{2R_2} \right)_{\text{evol,therm}} + \left(\frac{|J|}{J} \right)_{\text{MB,GR}} - \frac{|\dot{M}_{2,\text{evap}}|}{M_2} F(q, \xi_{\text{ad}}, \alpha_{\text{evap}}), \quad (20)$$

with

$$F(q, \xi_{\text{ad}}, \alpha_{\text{evap}}) = \frac{5}{6} + \frac{\xi_{\text{ad}}}{2} - \alpha_{\text{evap}} \frac{(1+q)}{q} - \frac{1}{3(1+q)}, \quad (21)$$

and the denominator is,

$$D = \frac{5}{6} + \frac{\xi_{\text{ad}}}{2} - \frac{1-\beta}{3(1+q)} - \frac{\alpha_{\text{RL}}(1-\beta)(1+q) + \beta}{q}. \quad (22)$$

As pointed out by Rappaport et al. (1983), stable mass transfer demands both the numerator and denominator of the right hand of Eq. (20) to be positive. If the denominator $D < 0$ then the mass transfer is dynamically unstable, while the system will become detached if the numerator is negative. The evaporative wind can either contribute to, or detract from, the star filling its RL, depending on the AM that it takes away. For stable mass transfer with $D > 0$, the evaporative wind adds a negative term $-\frac{|\dot{M}_{2,\text{evap}}|}{M_2} F(q, \xi_{\text{ad}}, \alpha_{\text{evap}})$ to the numerator, which tends to make the donor star underfill its RL eventually (as in the case of black widows). However, the details of evaporation are still not clear, in the following we will show how different values of α_{evap} can influence the binary evolution.

Finally, although the three transitional pulsars are only a small part of AMXPs, it is possible that active radio pulsars have indeed turned on during the quiescent state of LMXBs, even with no detected radio pulsations (Iacolina et al. 2010).

(2) The redback companions

Optical/infrared observations can reveal the evolutionary state of the redback companions and the nature of interacting binary systems. Statistically, most redbacks possess MS

companions which is under strong irradiation with spectral type changes or optical variability between inferior and superior conjunctions (Breton et al. 2013; Martino et al. 2014; Li et al. 2014). Other types of companion stars are also possible. For example, for the redback PSR J1740–5340 in NGC 6397, two scenarios were proposed to explain the inferred large mass loss rate from its companion, i.e. a MS star ablated by the MSP’s impinging flux or inhibited RLOF of an evolved star by the pulsar’s wind flux (D’Amico et al. 2001a,b; Ferraro et al. 2011). Ergma (2003) and Mucciarelli (2013) investigated the surface chemical abundances of its companion, and suggested the pulsar’s companion to be a deeply peeled evolved star. Additionally, PSR J1816+4510 may possess a (proto-)He WD companion, which is well within its RL (Kaplan et al. 2013). Therefore, the redback companions could be MS stars, evolved stars or (proto-)WDs. These features are compatible with the expectations in our formation scenario of redbacks.

The condition for the disk instability favors wide systems, and our calculations suggest that transient MSP-LMXB systems can form with orbital periods up to tens of days. It is interesting to note that the longest orbital period of known redbacks is 32.5 hours for PSR J1740–5340. By the way, all discovered AMXPs are distributed in a similar range of orbital periods, which are less than 1 day (Patruno & Watts 2012). So one would ask why there are no redbacks in wider orbits. This question is also related to the fact that transient LMXBs with orbital periods longer than 1 day have thus far been rare (Ritter & Kolb 2003; Kneivitt et al. 2014). Probably redbacks do possess giant companions, but their number is very small due to their short evolutionary times (Shao & Li 2015).

(3) Efficiency of irradiation and evaporation

Unlike CVs, there are few LMXBs with orbital period less than 4 hours, since X-ray irradiation of the donor star alters the long-term evolution of LMXBs (Kolb 1996). It might also be also responsible for the birthrates discrepancy between Galactic LMXBs and low-mass binary radio pulsars (Kulkarni & Narayan 1988). X-ray irradiation can affect the structure of the donor star by depressing its intrinsic luminosity. Podsiadlowski (1991) showed that spherically symmetric irradiation could expand the donor star and elevate the mass transfer rate, hence shortening the timescale of mass transfer (see however Nelson & Rappaport 2003). Hameury et al. (1993) investigated the situation of asymmetrical irradiation, and found that cyclic mass transfer was possible for a significant fraction of LMXBs, due to the irradiation instability (see also Ritter et al. 2000; Büning & Ritter 2004). Recently, Benvenuto et al. (2014, 2015) proposed that the redback companions should be quasi-RL filling stars during the detached episode of the cyclic mass transfer. The occurrence of the irradiation instability requires sustained strong irradiation over at least a thermal timescale of the convective envelope of the companion star, which is typically millions of years for a

low-mass MS star and much longer than the thermal-viscous timescale (less than years for compact binaries). The fact that reback systems are distributed in the thermal-viscous instability region, implies the irradiation instability may be suppressed in these binaries due to the intermittent irradiation (Ritter 2008).

The formation of eclipsing pulsars like black widows and rebacks also critically depends on the efficiency of evaporation of the companion star and related AML. In the literature, the proposed energy source of evaporation can be either the spin-down power of a MSP (Ruderman et al. 1989a) or the accretion power during the LMXB phase (Ruderman et al. 1989b), and we have only considered the former case in this work. van den Heuvel & van Paradijs (1988) first realized that MSP’s evaporation could account for the lack of LMXBs below the period gap. Therefore, to investigate the influence of the evaporation, we perform calculations of the LMXB evolution with $M_{2,i} = 1.0 M_{\odot}$ and different values of f^1 and AML modes. The results are shown in Fig. 5, in which the line styles and the symbols have the same meanings as in Fig. 3, and we add the black widow systems with data taken from A. Patruno’s catalogue². Also note that for ultra-compact systems the critical mass transfer rate for unstable disks should be replaced with those for He- or C/O-dominated disks (Menou et al. 2002; Lasota et al. 2008), but this actually causes very small change of the stable/unstable disk area.

In the upper, middle, and lower panels of Fig. 5, we assume that the evaporative wind takes the specific AM of the donor star (Mode A), at the inner Lagrangian point (Mode B), and in the extreme (non-physical) case with no AM (Mode C), while from left to right, we increase the value of f in each case. As we see from the figure, with decreasing specific AM of the evaporative wind, the binary eventually evolves to a wider orbit, the duration of RLOF is reduced, and the companion star is more likely to be detached from its RL. Obviously increasing the value of f results in a similar tendency. Smedley et al. (2015) showed that when $f \gtrsim 0.12$, evaporation is strong enough to keep the companion star detaches immediately in their AIC model. Our calculations indicate that whether the companion star can fill its RL heavily depends on the choice of the evaporation model: the donor star can detach immediately in some sequences of Modes B and C, while it can hardly detach after the start of evaporation in Mode A, even with a large value of f . The evaporation efficiency also affects the formation of ultra-compact systems below 0.1 day. For contracting systems, after the cessation of MB, GR-induced AML acts as a weak counterweight to the orbital expan-

¹The change in f reflects both the geometric effect and the variation in the initial spin-down power, which is fixed in the calculation.

²<https://apatruno.wordpress.com/about/millisecond-pulsar-catalogue/>

sion, so ultra-compact systems can be formed only with weak evaporation. Smedley et al. (2015) showed that, when $f < 0.044$ evaporation is not strong enough and the systems can reconnect for another phase of RLOF. Figure 5 reveals that this value of f also depends on the adopted AML modes, and the orbital evolution is much more sensitive to the values of f in Modes B and C than in Mode A.

(4) Will redbacks evolve to black widows?

According to Chen et al. (2013), black widows and redbacks are two distinct populations of eclipsing MSPs for different evaporation efficiencies due to the geometric effect. On the contrary, Benvenuto et al. (2014, 2015) argued that redbacks with compact orbits would evolve to black widows, while the ones with longer orbital periods would evolve to MSP-He WD systems. Basically, whether or not a redback can evolve to a black widow depends on two factors: (1) the evaporation efficiency, and (2) the balance between orbital expansion caused by mass transfer/loss and orbital contraction induced by AM carried away by the evaporative wind. Our calculations indicate that, for suitable choice of the f values, (at least some of) compact redbacks can evolve to black widows while the wide ones will form MSP-He WD systems in both Modes A and B.

6. SUMMARY

This work is motivated by the recent discovery that the three transitional pulsars are both redbacks and transient AMXPs. We then suggest the thermal and viscous instability in the accretion disks in LMXBs to be a possible mechanism for the formation of redbacks. We investigate the parameter space for the occurrence of the disk instability in the evolution of LMXBs, and the influence of evaporation on their secular evolution. Our results can be summarized as follows.

1. Almost all LMXBs are subject to the thermal and viscous instability and experience transient phase(s) sooner or later in their evolution. If the NSs have been spun up to millisecond periods, the reduction of the mass transfer rate during quiescence provides a plausible mechanism for switching on the pulsar activity and the formation of redbacks, besides the disrupted MB and irradiation instability models.

2. In this scenario, the redback companions can be MS stars, evolved stars, and (proto-)WDs with either filled or underfilled Roche-lobes.

3. Considering the influence of evaporation on the binary evolution, some fraction of redbacks evolving along the contracting tracks may become black widows, while the wide

ones may form MSP-He WD binaries. The final products are heavily dependent on the evaporation efficiency and the specific AM carried away with evaporative mass loss, both of which deserve further study.

We are grateful to an anonymous referee for constructive comments, and Hailiang Chen and Thomas Tauris for helpful discussions. This work was supported by the Natural Science Foundation of China under grant Nos. 11133001 and 11333004, the Strategic Priority Research Program of CAS under grant No. XDB09010200, and the Munich Institute for Astro- and Particle Physics (MIAPP) of the DFG cluster of excellence “Origin and Structure of the Universe”.

REFERENCES

- Ablimit, I., & Li, X.-D. 2015, *ApJ*, 800, 98
- Antoniadis, J. 2014, *ApJL*, 797, L24
- Archibald, A. M., Kaspi, V. M., Bogdanov, S., et al. 2010, *ApJ*, 722, 88
- Archibald, A. M., Stairs, I. H., Ransom, S. M., Kaspi, V. M., & Kondratiev, V. I. et al. 2009, *Science*, 324, 1411
- Archibald, A. M., Bogdanov, S., Patruno, A., et al. 2015, *ApJ*, 807, 62
- Backer, D. C., Kulkarni, S. R., & Heiles, C. et al. 1982, *Nature*, 300, 615
- Benvenuto, O. G., De Vito, M. A., & Horvath, J. E. 2014, *ApJL*, 786, L7
- Benvenuto, O. G., De Vito, M. A., & Horvath, J. E. 2015, *ApJ*, 798, 44
- Bhattacharya, D., & van den Heuvel E. P. J. 1991, *Phys. Rep.*, 203, 1
- Bogdanov, S. et al. 2014, *ApJ* in press (arXiv:1412.5145)
- Breton, R. P., van Kerkwijk, M. H., Roberts, M. S. E., et al. 2013, *ApJ*, 769, 108
- Büning, A., Ritter, H. 2004. *A&A*, 423, 281
- Burderi, L., Possenti, A., D’ntona, F., et al. 2001, *ApJ*, 560, L71
- Burderi, L., D’ntona, F., & Burgay, M. 2002, *ApJ*, 574, 325

- Burderi, L., Di Salvo, T., D'ntona, F., Robba, N. R., & Testa, V. 2003, *A&A*, 404, L43
- Chen, H.-L., Chen, X., Tauris, T. M. & Han, Z. 2013, *ApJ*, 775, 27
- D'Amico, N., Lyne, A. G., Manchester, R. N., Possenti, A., & Camilo, F. 2001a, *ApJ*, 548, L171
- D'Amico, N., Possenti, A., Manchester, R. N., et al. 2001b, *ApJ*, 561, L89
- Deller, A. T., Archibald, A. M., Brisken, W. F., et al. 2012, *ApJL*, 756, L25
- Deloye, C. J. 2008, in *AIP Conf. Proc.* 983, 40 years of Pulsars: Millisecond Pulsars, Magnetars and More, ed. C. Bassa, Z. Wang, A. Cumming, & V. M. Kaspi (Melville, NY: AIP), 501
- de Martino, D., Belloni, T., Falanga, M., et al. 2013, *A&A*, 550, A89
- de Martino, D., Falanga, M., Bonnet-Bidaud, J.-M., et al. 2010, *A&A*, 515, A25
- Demircan, O., & Kahraman, G. 1991, *Ap&SS*, 181, 313
- Dubus, G., Lasota, J.-P., Hameury, J.-M., & Charles, P. 1999, *MNRAS*, 303, 139
- Eggleton, P. P. 1971, *MNRAS*, 151, 351
- Eggleton, P. P. 1972, *MNRAS*, 156, 361
- Eggleton, P. P. 1983, *ApJ*, 268, 368
- Ergma, E., & Sarna, M. J. 2003, *A&A*, 399, 237
- Ferraro, F. R., Possenti, A., d'mico, N., & Sabbi, E. 2001, *ApJ*, 561, L93
- Ferrigno, C. et al, 2014, *A&A* ,567, A77
- Fruchter, A. S., Stinebring, D. R., & Taylor, J. H. 1988, *Natur*, 333, 237
- Grevesse, N., & Sauval, A. J. 1998, *SSRv*, 85, 161
- Hameury, J. M., King, A. R., Lasota, J. P., & Raison, F. 1993, *A&A*, 277, 81
- Iacolina, M. N., Burgay, M., Burderi, L., Possenti, A., & di Salvo, T. 2010, *A&A*, 519, A13
- Iben I., Tutukov A. V., Yungelson L. R., 1995, *ApJS*, 100, 233
- Illarionov, A., & Sunyaev, R. 1975, *A&A*, 39, 185

- Jia, K., & Li, X.-D. 2014, *ApJ*, 791, 127
- Joss, P. C., Rappaport, S. A., & Lewis, W. 1987, *ApJ*, 319, 180
- Kaplan, D. L., Bhalariao, V. B., van Kerkwijk, M. H., Koester, D., Kulkarni, S. R. & Stovall, K., 2013, *ApJ*, 765, 158
- King, A. R., Frank, J., Kolb, U., & Ritter, H. 1995, *ApJ*, 444, L37
- King, A. R., Frank, J., Kolb, U., & Ritter, H. 1996, *ApJ*, 467, 761
- King, A. R., Frank, J., Kolb, U., & Ritter, H. 1997, *ApJ*, 484, 844
- King, A. R., & van Teeseling, A. 1998, *A&A*, 338, 965
- King, A. R., Rolfe, D. J., Kolb, U., & Sshenker, K. 2003, *MNRAS*, 341, L35
- Knevitt G., Wynn G. A., Vaughan S., Watson M. G., 2014, *MNRAS*, 437, 3087
- Kulkarni, S. R., & Narayan, R. 1988, *ApJ*, 335, 755
- Kolb, U. 1996, in *IAU Colloq. 158, Cataclysmic Variables and Related Objects*, ed. A. Evans & J. H. Wood (Dordrecht: Kluwer), 433
- Landau, L. D., & Lifshitz, E. M. 1975, in *Course of Theoretical Physics Pergamon International Library of Science, Technology, Engineering and Social Studies* (4th rev. Engl. ed.; Oxford: Pergamon)
- Lasota, J.-P., Dubus, G., & Kruk, K. 2008, *A&A*, 486, 523 Lasota, J. P. 2001, *New Astronomy Review* 45, 449
- Li, M., Halpern, J. P., & Thorstensen, J. R. 2014, *ApJ*, 795, 115
- Lin, J., Rappaport, S., & Podsiadlowski, P. et al. 2011, *ApJ*, 732, 70
- Linares, M. 2014, *ApJ*, 795, 72
- Linares, M. et al. 2014, *MNRAS*, 438, 251
- Lipunov, V. M., & Postnov K. A., 1984, *Ap&SS*, 106, 103
- Ma, B., & Li, X.-D. 2009, *ApJ*, 691, 1611

- Martino R., Mazzotta P., Bourdin H., Smith G. P., Bartalucci I., Marrone D. P., Finoguenov A., Okabe N., 2014, MNRAS, 443, 2342
- Menou, K., Perna, R., & Hernquist, L. 2002, ApJL, 564, L81
- Mucciarelli, A., Salaris, M., Lanzoni, B., et al. 2013, ApJL, 772, L27
- Nelson, L. A., & Rappaport, S. 2003, ApJ, 598, 431
- Papitto, A., Ferrigno, C., & Bozzo, E., et al. 2013, Natur, 501, 517
- Papitto, A. et al. 2015, MNRAS, 449, L26
- Patruno, A. et al. 2014, ApJ, 781, L3
- Patruno, A., & Watts, A. L. 2012, arXiv:1206.2727
- Paxton, B., Bildsten, L., Dotter, A., et al. 2011, ApJS, 192, 3
- Paxton, B., Cantiello, M., Arras, P., et al. 2013, ApJS, 208, 4
- Paxton, B., Marchant, P., Schwab, J., et al. 2015, arXiv:1506.03146
- Podsiadlowski, P. 1991, Natur, 350, 136
- Podsiadlowski, P., Rappaport, S., & Pfahl, E. D. 2002, ApJ, 565, 1107
- Pringle, J. E., & Rees, M. J. 1972, A&A, 21, 1
- Pylyser, E. H. P., & Savonije, G. J. 1988, A&A, 191, 57
- Pylyser, E. H. P., & Savonije, G. J. 1989, A&A, 208, 52
- Rappaport, S., Verbunt, F., & Joss, P. C. 1983, ApJ, 275, 713
- Rappaport, S., Podsiadlowski, Ph., Joss, P. C., Di Stefano, R., & Han, Z. 1995, MNRAS, 273, 731
- Ritter, H. 1988, A&A, 202, 93
- Ritter, H. 2008, NewAR, 51, 869
- Ritter H., & Kolb U., 2003, A&A, 404, 301
- Ritter, H., Zhang, Z., & Hameury, J.-M. 1996, in Cataclysmic variables and related objects, ed. A. Evans, & J. H. Wood, IAU Coll. 158 (Dordrecht: Kluwer Academic Publishers)

- Ritter, H., Zhang, Z., & Kolb, U. 1995, in *Cataclysmic variables*, ed. A. Bianchini, M. della Valle, & M. Orio (Dordrecht: Kluwer Academic Publishers), 479
- Ritter, H., Zhang, Z.-Y., & Kolb, U., 2000. *A&A* 360, 969.
- Roberts, M. S. E. 2013, in *Proc. IAU Symposium, Vol. 291, Neutron Stars and Pulsars*, ed. J. van Leeuwen (Cambridge: Cambridge Univ. Press), 127
- Roy, J., Bhattacharyya, B., & Ray, P. 2014, *ATel*, 5890, 1
- Ruderman, M., Shaham, J., & Tavani, M. 1989a, *ApJ*, 336, 507
- Ruderman, M., Shaham, J., Tavani, M., & Eichler, D. 1989b, *ApJ*, 343, 292
- Shao, Y., & Li, X.-D. 2012, *ApJ*, 756, 85
- Shao, Y., & Li, X.-D. 2015, *ApJ*, submitted
- Shapiro, S. L., & Teukolsky, S. A. 1983, *Black Holes, White Dwarfs, and Neutron Stars: The Physics of Compact Objects* (New York: Wiley)
- Smedley, S. L., Tout, C. A., & Ferrario, L. 2015, *MNRAS*, 446, 2540
- Spruit, H. C., & Ritter, H. 1983, *A&A*, 124, 267
- Stappers, B. W., Bailes, M., Lyne, A. G., et al. 1996, *ApJL*, 465, L119
- Stappers, B. W. et al. 2014, *ApJ*, 790, 39.
- Stevens, I. R., Rees, M. J. & Podsiadlowski, P., 1992, *MNRAS*, 254, 19P
- Tauris, T. M. 2012, *Science*, 335, 561
- Tauris, T. M., Langer, N., & Kramer, M. 2012, *MNRAS*, 425, 1601
- Tauris, T. M., & Savonije, G. J. 1999, *A&A*, 350, 928
- van den Heuvel, E. P. J., & van Paradijs, J. 1988, *Natur*, 334, 227
- van Kerkwijk, M. H., Breton, R. P., & Kulkarni, S. R. 2011, *ApJ*, 728, 95
- Verbunt, F., & Zwaan, C. 1981, *A&A*, 100, L7
- Wijnands & van der Klis, 1998, *Natur*, 394, 344
- Zhang, C. M., Wang, J., Zhao, Y. H., et al. 2011, *A&A*, 527, A83

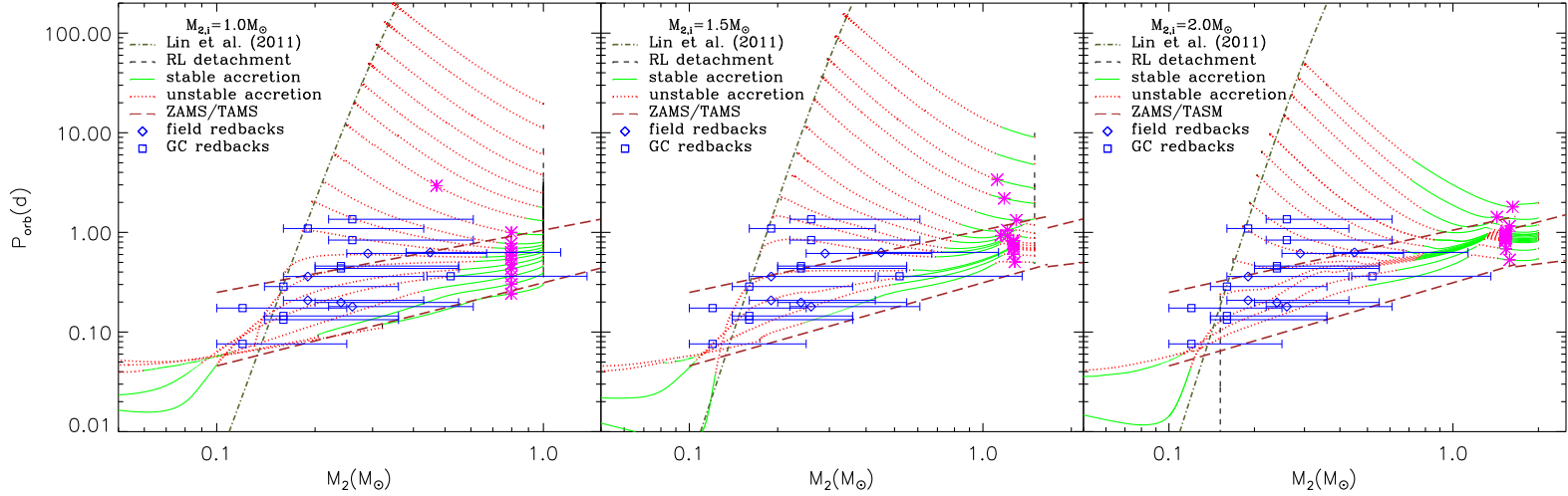


Fig. 1.— Evolutionary tracks of LMXBs in the $M_2 - P_{\text{orb}}$ plane. From left to right the initial masses of the companion stars are taken to be $M_{2,i} = 1.0, 1.5,$ and $2.0 M_{\odot}$, respectively. The green solid, red dotted, and black dotted lines represent the mass transfer processes with a stable and unstable accretion disk, and the stage of RL detachment, respectively. The dotted-dashed line shows the theoretical $P_{\text{orb}} - M_{\text{WD}}$ relation for case B mass transfer. The asterisks on the evolutionary tracks indicates the time when the NS has accreted $0.1M_{\odot}$ material. The two **brown** dashed lines give the orbital periods with a ZAMS and TAMS donor. Also plotted are rebackscatters in the Galactic disk and globular clusters with blue symbols.

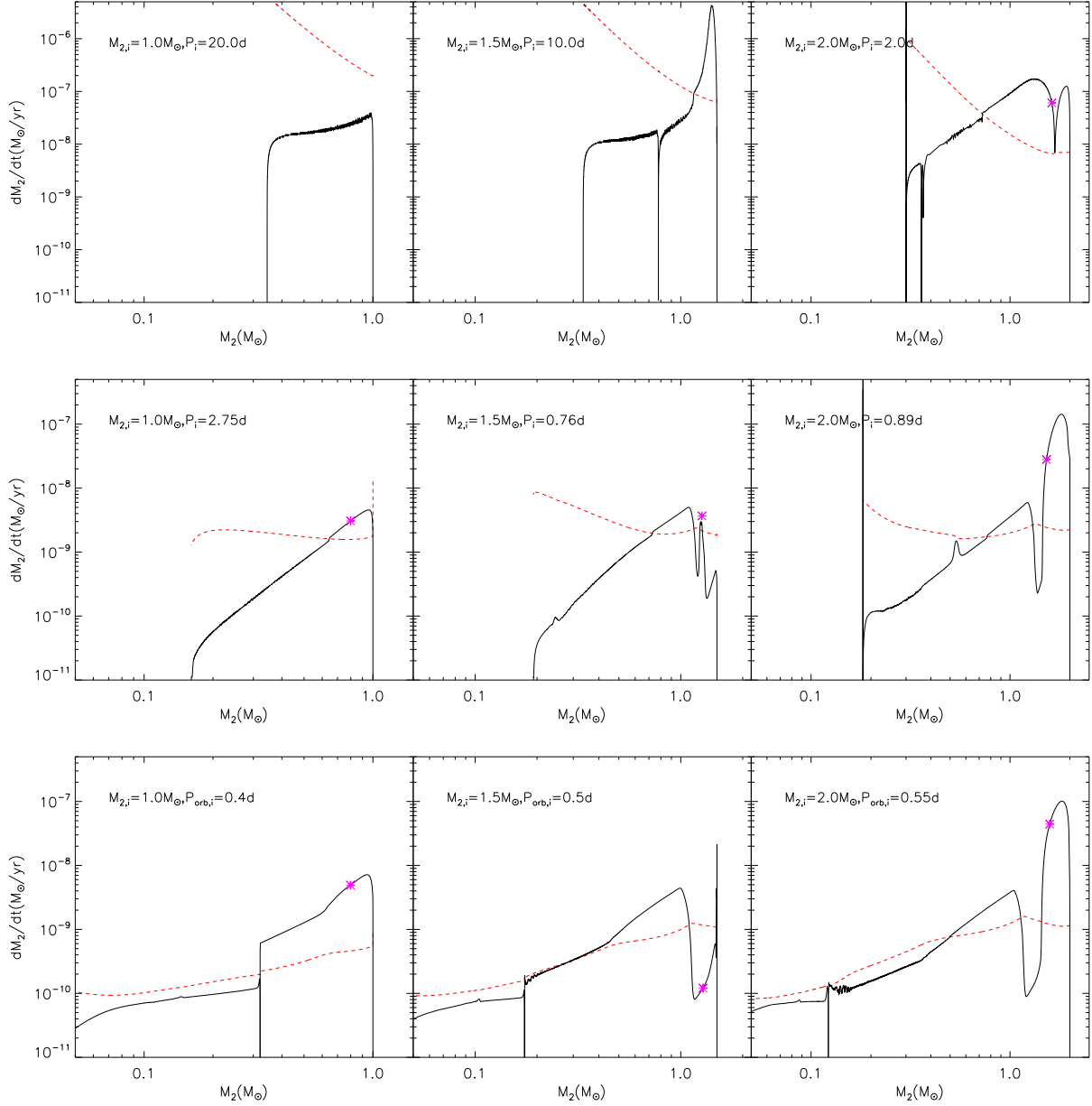


Fig. 2.— The mass transfer rate through RLOF (black solid line) and the critical accretion rate for disk instability (red dashed line) as a function of the donor mass. The bottom to top rows show **contracting** to **widening** evolutionary tracks with increasing initial orbital periods. In the left, middle, and right columns the initial donor masses are $M_{2,i} = 1.0, 1.5,$ and $2.0 M_\odot$, respectively. The asterisk indicates when the NS has accreted $0.1 M_\odot$ material.

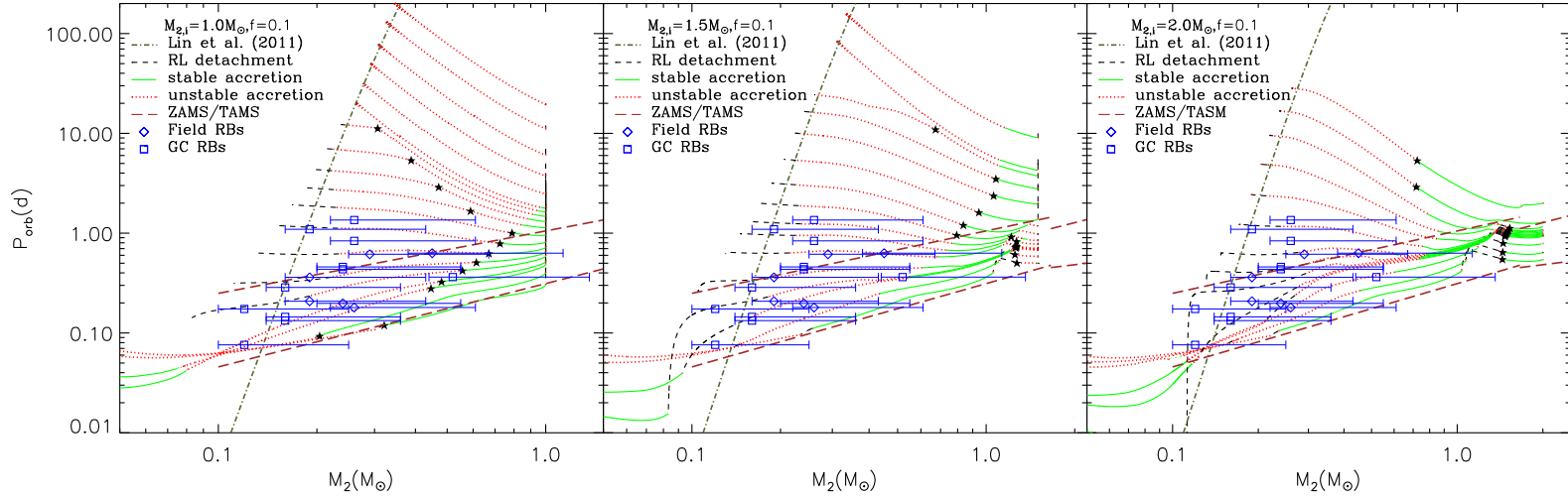


Fig. 3.— Similar to Fig. 1 but with evaporation taken into account ($f = 0.1$). The beginning of evaporation is labeled with a solid pentagram.

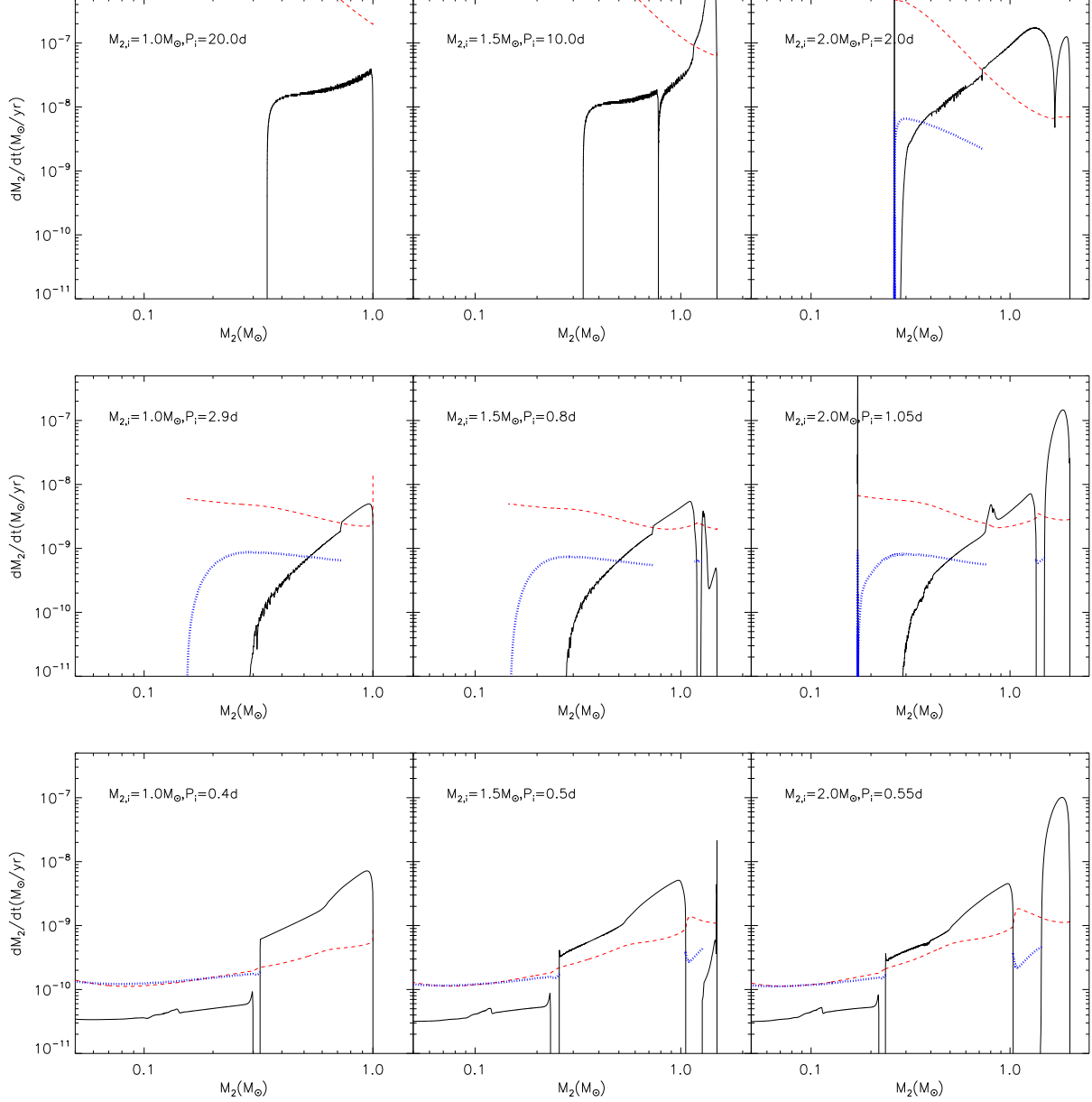


Fig. 4.— Similar to Fig. 2 but with evaporation taken into account ($f = 0.1$). The mass loss rate caused by evaporation is plotted with the blue dotted lines.

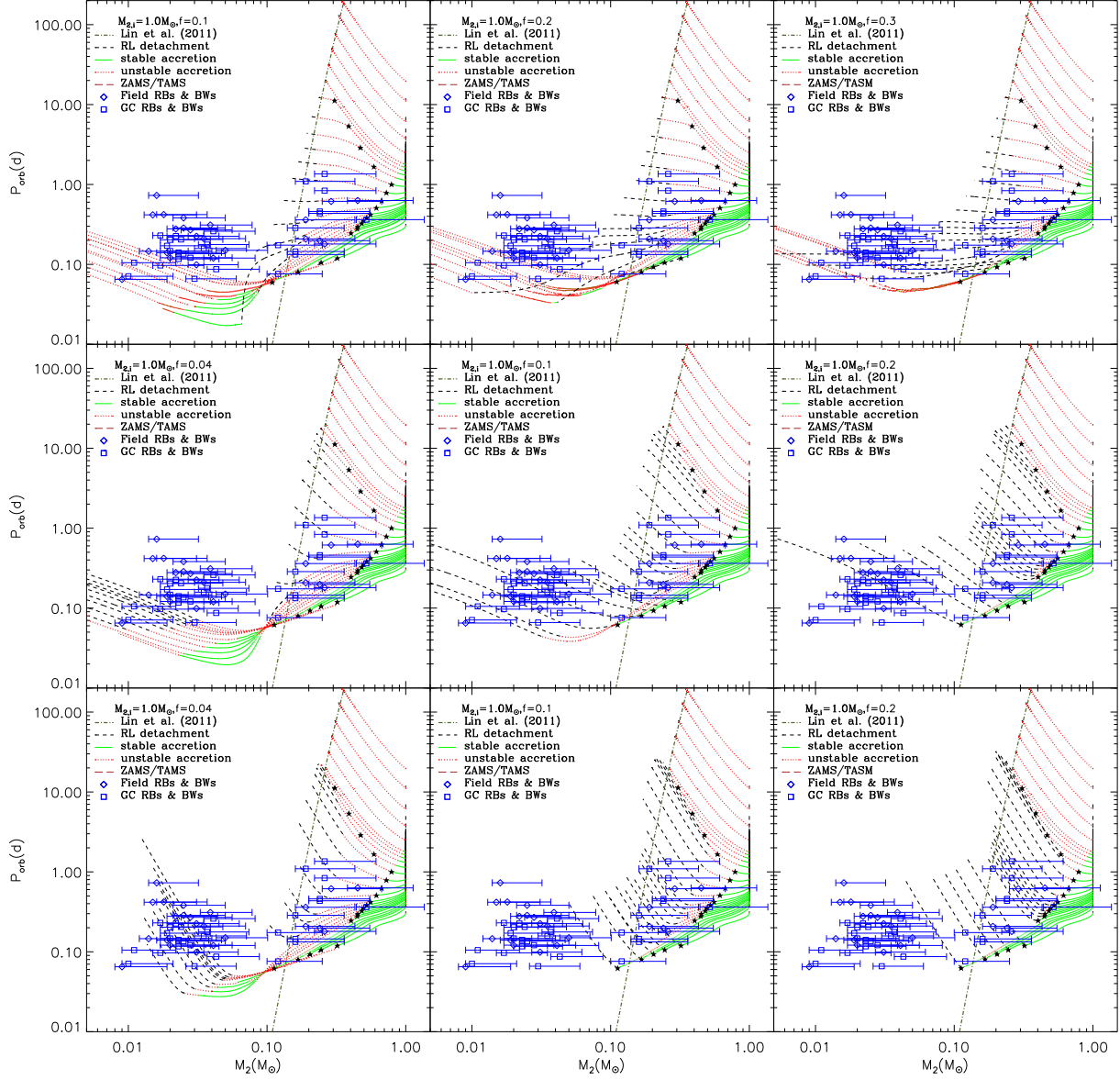


Fig. 5.— Similar to Fig. 3 but with various efficiency and AML modes of the evaporative wind. From top to bottom rows, the evaporative wind is assumed to carry the specific angular momentum of the donor star (Mode A), at the inner Lagrangian point (Mode B), and no AM (Mode C) respectively. The evaporation efficiency is taken to be $f = 0.1, 0.2,$ and 0.3 for Mode A, and $0.04, 0.1,$ and 0.2 for Modes B and C. Also plotted are black widow systems in the Galactic field (Field BWs) and globular clusters (GC BWs) with blue symbols.